Journal of Colloid and Interface Science 607 (2022) 1754–1761

Contents lists available at ScienceDirect

Journal of Colloid and Interface Science

journal homepage: www.elsevier.com/locate/jcis

pH effects on the molecular structure and charging state of β-Escin biosurfactants at the air-water interface

Dana Glikman [a], Natalia García Rey [a], Manuela Richert [a], Konrad Meister [b,c], Björn Braunschweig [a,*]

[a] Institute of Physical Chemistry and Center for Soft Nanoscience, Westfälische Wilhelms-Universität Münster, Corrensstraße 28/30, Münster 48149, Germany
[b] Max Planck Institute for Polymer Research, Mainz 55128, Germany
[c] University of Alaska Southeast, Juneau, AK 99801, United States

GRAPHICAL ABSTRACT

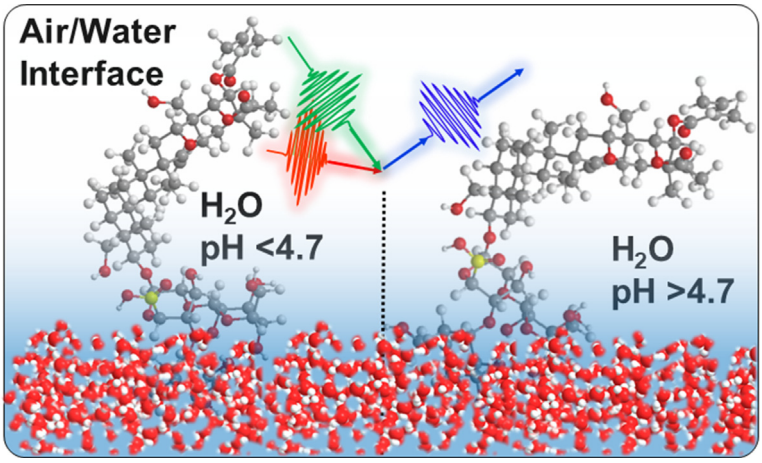

ARTICLE INFO

Article history:
Received 12 April 2021
Revised 24 July 2021
Accepted 17 September 2021
Available online 20 September 2021

ABSTRACT

Saponins like β-escin exhibit an unusually high surface activity paired with a remarkable surface rheology which makes them as biosurfactants highly interesting for applications in soft matter colloids and at interfaces. We have applied vibrational sum-frequency generation (SFG) to study β-escin adsorption layers at the air-water interface as a function of electrolyte pH and compare the results from SFG spectroscopy to complementary experiments that have addressed the surface tension and the surface dilational rheology. SFG spectra of β-escin modified air-water interfaces demonstrate that the SFG intensity of O—H stretching vibrations from interfacial water molecules is a function of pH and dramatically increases when the pH is increased from acidic to basic conditions and reaches a plateau at a solution pH of > 6. These changes are attributable to the interfacial charging state and to the deprotonation of the carboxylic acid group of β-escin. Thus, the change in O—H intensity provides qualitative information on the degree of protonation of this group at the air-water interface. At pH < 4 the air-water interface is dominated by the charge neutral form of β-escin, while at pH > 6 its carboxylic acid group is fully deprotonated and, consequently, the interface is highly charged. These observations are corroborated by the change in equilibrium surface tension which is qualitatively similar to the change in O—H intensity as seen in the SFG spectra. Further, once the surface layer is charge neutral, the surface elasticity drastically increases. This can be attributed to a change in prevailing intermolecular interactions that change from

* Corresponding author.
E-mail address: braunschweig@uni-muenster.de (B. Braunschweig).

https://doi.org/10.1016/j.jcis.2021.09.086

dominating repulsive electrostatic interactions at high pH, to dominating attractive interactions, such as hydrophobic and dispersive interactions, as well as, hydrogen bonding at low pH values. In addition to the clear changes in O—H intensity from interfacial H_2O, the SFG spectra exhibit drastic changes in the C—H bands from interfacial β-escin which we relate to differences in the net molecular orientation. This orientation change is driven by tighter packing of β-escin adsorption layers when the β-escin moiety is in its charge neutral form (pH < 4).

1. Introduction

β-escin is the main component of escin which is a mixture of saponins that can be extracted from the horse chestnut tree (*Aesculus hippocastanum*). β-escin is considered as a natural occurring biosurfactant with well-documented anti-inflammatory and other medicinal properties,[1,2] but also exhibits remarkable elastic properties at the air-water interface.[3–6] This has triggered great interest in the application of saponins as surfactants e.g. for stabilization of foams and emulsions.[4,7–11] Some of them have been recently reviewed by Hellweg and co-workers.[12]

On one hand, the interfacial and bulk structure e.g. of escin has been well established by small-angle X-ray scattering,[13,14] neutron reflectometry[7,15,16] as well as by molecular dynamic simulation.[9,17] On the other hand, this is different for the interfacial charging state of saponins e.g. at air-water interfaces, where a detailed molecular understanding is still missing or incomplete, as it is often inferred from bulk properties. Some studies on interfacial properties of β-escin at different pH of the aqueous solution already exist. For instance, Penfold et al.[7] reported that β-escin forms closely-packed adlayers at the air-water interface and demonstrate that the hydrophobic part of β-escin is orientated towards the gas phase and exhibits a thickness of 0.8 nm, that is much smaller as expected from the molecular structure (1.4 nm). (See Fig. 1.) Consequently, this points to a partial immersion of the hydrophobic scaffold in the solvent subphase and/or a tilt of the hydrophobic scaffold at the interface, which is both consistent with predictions from molecular dynamic simulations.[9,17] The thickness of the hydrophilic oligosaccharide part of β-escin in the aqueous phase is 1.4 nm with a high volume fraction (0.8) of the saponin, which is further evidence for the tight packing of β-escin at the air-water interface.[7,17] In addition to the interfacial structure, Penfold et al.[7] have also addressed the surface excess of β-escin for the two selected pH values 4 and 8. At concentrations > 60 μM, which is attributed to the critical micelle concentration (cmc) of β-escin, the surface excess of 2 $\mu mol/m^2$ showed little changes with pH and concentration, as expected for concentrations > cmc. For concentrations well below the cmc, however, the surface excess was drastically different between pH 4 and 8. This behavior was ascribed to a possible charging behavior of β-escin at an interface and in the bulk solution and was attributed to the carboxylic acid group that is located in the glycone; which is the oligosaccharide part of β-escin as opposed to the aglycone – the hydrophobic scaffold (see Fig. 1).

The *pK* = 4.7 of the carboxylic acid group has recently been determined by Dargel et al.[18] by titrating the bulk solution and it is, thus, reported that the carboxylic acid group of β-escin is in the bulk protonated at pH ≪4.7, while at pH > 4.7, the group is either partially or fully ionized. Using the autofluorescence of β-escin, Dargel et al. also reported the cmc of β-escin in a 50 mM phosphate buffer at pH 7.4 to be at 330 μM.[18]

The bulk charging behavior is in good agreement with the interfacial changes as function of pH (see above), although interface charging is not in many studies addressed for the full pH range. Clearly, interface adsorption of β-escin at a pH > 4.7 can lead to surface charging and the formation of an interfacial electric double layer, but the different charging states of β-escin can also lead to different interfacial structures. This was predicted by MD simulations where for the β-escin moiety with the deprotonated carboxylic acid forms a buckled adsorbate layer, while the neutral moiety tends to form a more uniform and flat adlayer.[9] The interfacial properties of β-escin that change with pH can have also far

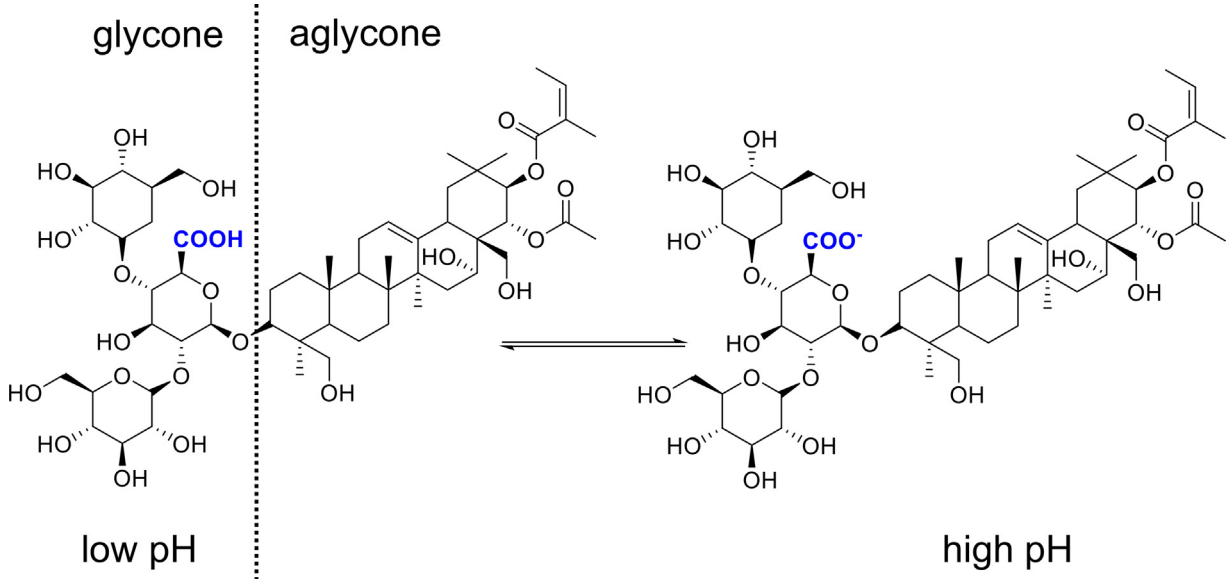

Fig. 1. Chemical structure of a protonated and deprotonated β-escin molecule, which consists of a hydrophobic scaffold - the aglycone - and a hydrophilic oligosaccharide part which is called the glycone. The ionizable carboxylic acid group is highlighted in blue color.

reaching consequences as for instance the gas permeability of β-escin-stabilized aqueous foam changes drastically with pH, which is attributed to the high resistance of β-escin adsorption layer to gas diffusion.[8]

As the pH causes different interfacial charging and packing of the adsorption layers[9] the physical properties, e.g. in their role as a gas diffusion barrier, can drastically change foam coarsening. Therefore, it is interesting to study the surface charging of β-escin interfacial layers in much greater detail. For that reason, we have applied vibrational sum-frequency generation spectroscopy and complementary pendant drop experiments to determine both the interface tension and surface dilatational rheology as well as the interfacial charging through the use of SFG spectroscopy. This multi-technique approach has enabled us to study the molecular structure of β-escin adsorption layers as well as pH induced surface charging and molecular orientation at the air-water interface.

2. Experimental details

2.1. Sample preparation

β-escin (CAS 11072–93-8, purity > 95 %) was obtained from Santa Cruz Biotechnology (USA) and was used as received. In order to avoid issues with the solubility of β-escin surfactants and to keep the surfactant concentration well below cmc, we prepared all samples at a fixed concentration of 25 μM. β-escin was dissolved in ultrapure water (18.2 M Ωcm; total oxidizable carbon ≤ 3 ppb), which was taken from a Merck Milli-Q Reference A + purification system, and was sonicated for at least 5 h to make sure that it was fully dissolved. The temperature of the water in the sonication bath (max. 60 W, 45 kHz) was continuously checked and it was made sure that the temperature was always below 30 °C. Before the experiments, 3 mL of the solution were additionally filtered through a 1 μm syringe-filter and aliquots of aqueous HCl or NaOH solutions were added to adjust the bulk pH to values between 2 and 12. All measurements were performed at 297 K room temperature using freshly prepared and pH adjusted solutions. The glassware for preparing samples and for the measurements was immersed for at least 12 h in a mixture of concentrated sulfuric acid (98 %, Rotipuran by Carl Roth, Germany) and Nochromix (Godax Labs, USA) and was subsequently thoroughly rinsed with copious amounts of ultrapure water.

3. Surface tensiometry and dilational rheology

The surface tension was measured using a pendant drop tensiometer (PAT-1 M, Sinterface Germany) and drop shape analysis. For that, a drop with a volume of 15 mm^3 was created and the drop shape was monitored and analyzed using Young-Laplace equation. After the surfaces reached an equilibrium, which was roughly the case after an adsorption time of 7200 s, harmonic surface area oscillations were applied at a frequency of 0.1 Hz and the degree of the area deformation of $\Delta A/A$ 8% and the surface tension response were recorded. Using Fourier transformation from the drop shape and surface tension changes, the dilatational complex visco-elasticity modulus $|E|$ were determined as described in detail elsewhere.[19] Note that the times we have left the samples to equilibrate is sufficiently larger than the characteristic adsorption times e.g. for Quillaja saponins which were reported by Stanimirova et al.[20], but similar to what Giménez-Ribes et al.[6] have reported for escin (2400 s). Stanimirova et al.[20] also pointed out that drop shape analysis can lead to systematically lower surface elasticities when adsorption layers give rise to very high elasticities e.g. in the case of saponins at air-water interfaces. These likely originate from the much slower relaxation times for adsorption/desorption and structural rearrangement of saponins at the air-water interface. For the typical (low) frequency of an oscillating drop experiment the systems slow response thus leads to the above described systematic deviations. For that reason, we have additionally performed experiments where the drop area was slowly inflated after an initial waiting time. We note that the method is similar to what Ulaganathan et al. [21] have used in their study of Quillaja bark saponin. In particular, we have set the drop volume to 12 mm^3 for 7200 s to equilibrate the surface and subsequently expanded the drop volume within 100 s to yield an maximum surface area increase by 35 %. Next we plotted the interface tension γ (here equivalent to the surface stress σ) as a function of the area expansion $\alpha = (A_t - A_0)/A_0$ with A_t being the surface area at a given time t during expansion and A_0 the initial surface area before the drop was expanded. These $\sigma(\alpha)$ plots are shown in Fig. S1 of the Supporting Information from which we have determined the surface elasticity (shear modulus) G_s. For the analysis, we have selectively used the linear regime with low deformation of the pendant drop and where an isotropic strain field persist which gives rise to a simple linear relation $\sigma = G_s\alpha$ between the surface stress and the area expansion (see also previous detailed works e.g. [21,22]). We point out that in our study we are only interested in a very qualitative relation between surface charging, surface rheology and interface tension.

4. Sum-frequency generation spectroscopy (SFG)

Sum-frequency generation spectroscopy (SFG) is a second-order nonlinear spectroscopy that can be applied to study surfaces and interfaces of materials with inversion symmetry such as isotropic liquids and gases.[23] For vibrational SFG spectroscopy a frequency-tunable IR beam (ω_{IR}) and a visible beam at a fixed frequency (ω_{vis}) are overlapped in time and space at an interface, where a third beam with the sum frequency (SF) $\omega_{SF} = \omega_{IR} + \omega_{vis}$ of the two impinging beams is generated. The intensity of the sum-frequency signal is directly proportional to the square of the effective second-order electric susceptibility $\chi^{(2)}_{eff}$, which combines the nonresonant contribution $\chi^{(2)}_{NR}$, the resonant contribution of the surface $\chi^{(2)}_{R}$ and the resonant contribution of the electric double-layer $\chi^{(3)}_{R,EDL}$:[24–26]

$$I_{SF} \propto \left|\chi^{(2)}_{eff}\right|^2 = \left|\chi^{(2)}_{NR} + \chi^{(2)}_{R} + \chi^{(3)}_{R,EDL}\right|^2 \quad (1)$$

$\chi^{(2)}_{NR}$ is dominated by electronic excitations at the interface and often negligible for surfactant modified or neat air-water interfaces,[25] while $\chi^{(2)}_{R}$ originates from molecular vibrations. [23,27,28] The oscillator strength $A_q = N\langle\alpha_q\mu_q\rangle$ of these vibrations is a function of the number of adsorbed molecules N, the orientational average of the Raman polarizability α_q and the dynamic dipole moment μ_q. This orientational average consequently becomes zero in the bulk solution, rendering SFG inherently interface-specific for the air-water interface, as well as for other interfaces of isotropic materials. The contribution from the electric double-layer $\chi^{(3)}_{R,EDL}$ becomes significant when charged molecules are adsorbed to the interface and generate an additional static electric field.[24–26,29–31] In that case, the field-induced polarization and orientation of interfacial water molecules lead to an enhanced SF intensity that depends on the Debye length κ^{-1} (and consequently on the ionic strength), the wave vector mismatch Δk_z and the double-layer potential ϕ_0, which is a function of the interfacial charging state.

$$I_{SF} \propto \left| \chi^{(2)}_{NR} + \sum_q \frac{A_q e^{i\theta}}{\omega_q - \omega_{IR} + i\Gamma_q} + \frac{\kappa}{\kappa + i\Delta k_z} \chi^{(3)} \phi_0 \right|^2 \quad (2)$$

This means that the intensity of the vibrations of interfacial water molecules can be linked qualitatively, and – under certain conditions – also quantitatively to the double-layer potential.[25]

The set-up for our home-built SFG spectrometer is described in detail elsewhere. [25] In brief, we use a Spectra Physics (USA) Solstice Ace amplifier system that produces 70 fs pulses using an internal beam splitter: ~3.4 mJ pulse energy are taken to pump a Light Conversion TOPAS Prime optical parametric amplifier (OPA) and a subsequent unit for noncollinear difference-frequency generation of the signal and idler photons from the OPA. This provides mid-IR tunable femtosecond pulses with a bandwidth of > 300 cm^{-1}. The visible pulse (VIS) is generated by spectral narrowing of the 70 fs pulse from the Solstice Ace amplifier with an air-spaced etalon (SLS OPTics LTD, FSR 12.4 nm at 735 nm, R = 94.5%). This provides time-asymmetric pulses with a bandwidth of < 5 cm^{-1} at a wavelength of 804.1 nm. In our experiments, the VIS and IR pulses overlap in time and space at 55° and 60° incident angles and are focused to beam diameters of 530 and 260 μm, respectively. For SFG spectroscopy at the air-water interface, IR and VIS pulses with pulse energies of 15 μJ were used. SF photons were collected in a reflection geometry and guided to an Andor Kymera spectrograph with a 1200 lines/mm grating, where they are spectrally dispersed and subsequently detected with an Andor Newton EMCCD. SFG spectra in the frequency region from 2700 to 3800 cm^{-1} were taken by tuning the IR center frequency in four steps. The acquisition time for each center frequency was 180 s and the IR, VIS and SF beams were set to SSP polarizations. Normalization of the SFG spectra was done with the nonresonant contribution from a Au thin film on a Si wafer, which was cleaned in an air-plasma prior to each experiment.

5. Results

In Fig. 2, we present vibrational SFG spectra of β-escin modified air-water interfaces as a function of the bulk pH value. SFG spectra in Fig. 2 are dominated by two broad O—H stretching bands at ~ 3200 and ~ 3450 cm^{-1} which have been previously assigned to differently coordinated but hydrogen bonded interfacial water molecules. The low frequency branch of the O—H spectrum is often attributed to more tetrahedrally coordinated water molecules which some authors[28] also refer to as 'ice-like' interfacial water, while the high frequency branch is referred to as 'liquid-like' interfacial water due to a presumably more disordered (non-tetrahedral) H_2O coordination and weaker hydrogen bonds that reduce the red-shift in O—H stretching frequency, as compared to the frequency of free or dangling interfacial O—H groups at 3700 cm^{-1}.[28,32] At very acidic pH, a third but much weaker O—H band at 3600 cm^{-1} can be noticed, which gets overwhelmed by the much stronger bands at lower frequency when the pH is higher (see Fig. 3). In previous works,[33–35] a O—H band at a similar frequency was attributed to weakly hydrogen-bonded water molecules close to carbonyl groups at lipid-covered surfaces. For that reason, we assign the weak O—H band centered at 3600 cm^{-1} to weakly hydrogen-bonded water molecules close to the carbonyl and hydroxyl groups at the glycone of β-escin. This is highlighted in Fig. 3 where we compare SFG spectra taken at low and high pH values.

In addition to the broad O—H bands, much narrower bands at IR frequencies below 3100 cm^{-1} can be also observed in Figs. 2 and 3. They are attributable to C—H modes of interfacial β-escin molecules. The exact origin of these bands and of the apparent changes of C—H bands will be discussed in more detail below, because we

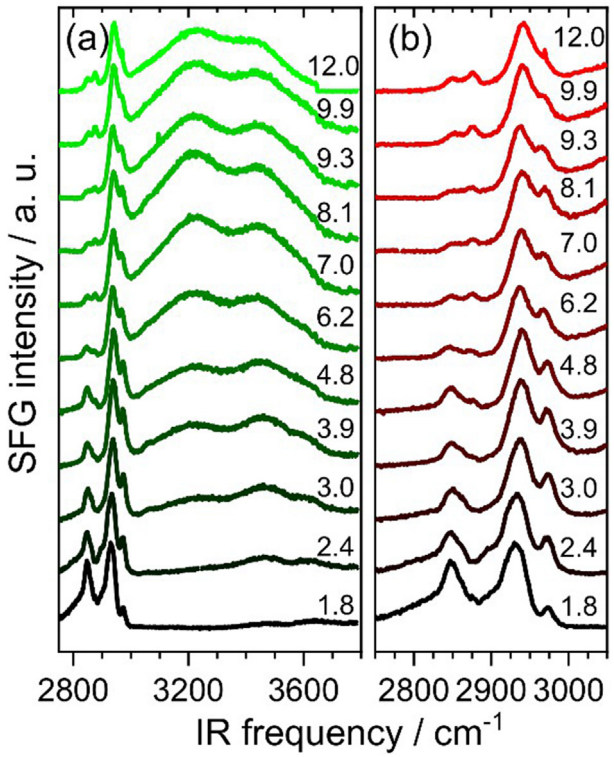

Fig. 2. Vibrational SFG spectra of β-escin (25 μM) modified air-water interfaces as a function of the pH of the aqueous solutions as indicated in the figure. Broad bands are due to O—H stretching vibrations of interfacial water while narrow bands (<3100 cm^{-1}) originate from C—H vibrations of interfacial β-escin as outlined in the main text.

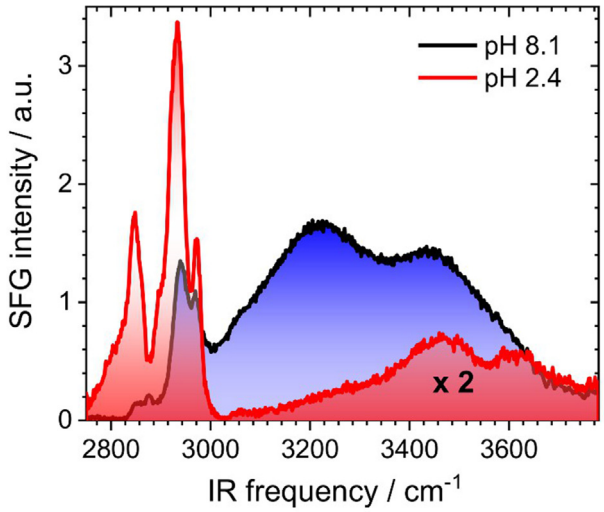

Fig. 3. Vibrational SFG spectra of the modified air-water interface with β-escin (25 μM) comparing the O—H stretching and C—H bands for low and high bulk pH values. The pH was as indicated in the figure. Note that the SFG spectrum which was taken at pH 2.4 was multiplied by a factor of 2.

first want to focus our discussion on the changes of the O—H bands in the SFG spectra of Fig. 2 as a function of solution pH. Clearly, there is a drastic dependence of the O—H intensity with pH.

Close inspection of Fig. 2 shows that for pH < 6.2 the O—H intensity decreases substantially as the pH gets more acidic until the O—H intensity is extremely low and the bands can be hardly noticed in the SFG spectra taken at pH of 2.4, where the C—H bands

dominate the SFG spectra. For pH > 4, the SFG intensity of the O—H bands first increases, then reaches a plateau and finally decreases again at very high pH. In order to address the changes of the O—H intensity with pH in a more quantitative fashion, we have fitted the SFG spectra in Fig. 2 with model functions which are described in detail in the Supporting Information.

In Fig. 4, we present both the SFG amplitude of the CH_2 symmetric stretching mode, that is discussed below, and the averaged amplitude of all O—H bands that we have to assume for this system (see above). From Fig. 4b, we can now infer that the plateau in O—H amplitude is reached at pH 4.8. Further, from an analysis of Fig. 4 we can also conclude that the changes in O—H intensity (Fig. 4b), equilibrium interface tension (Fig. 4c) and of the surface dilatational visco-elasticity (Fig. 4d) are highly correlated.

At this point we recall that the SFG intensity of interfacial water molecules can be strongly dependent on a so-called double layer contribution $\chi^{(3)}\phi_0$ (see experimental section), which depends on the third-order susceptibility $\chi^{(3)}$ and the double-layer potential ϕ_0. As discussed in the introduction, it is known that the carboxylic acid group of β-escin can be deprotonated at sufficiently high pH. In fact, the pK of the carboxylic acid group of β-escin moieties in the bulk solution was determined to be at 4.7 ± 0.2 by titration. [18] Hence, we conclude that the changes in O—H intensity with solution pH are directly related to the surface charging behavior of the β-escin moieties at the air-water interface and, thus, to the changes in the double-layer potential ϕ_0. Further, the plateau in O—H intensity and equilibrium surface tension that we observe in Figs. 2 and 4 are attributed to the interfacial pK of the adsorbate layer and that at pH > 6 the carboxylic acid groups of interfacial β-escin molecules are fully ionized. Thus, a further increase in pH cannot lead to additional charging at the interface, but rather to charge screening as with an increase in pH also the ionic strength of the aqueous solution increases. This causes the O—H amplitude and the surface tension to decrease slightly.

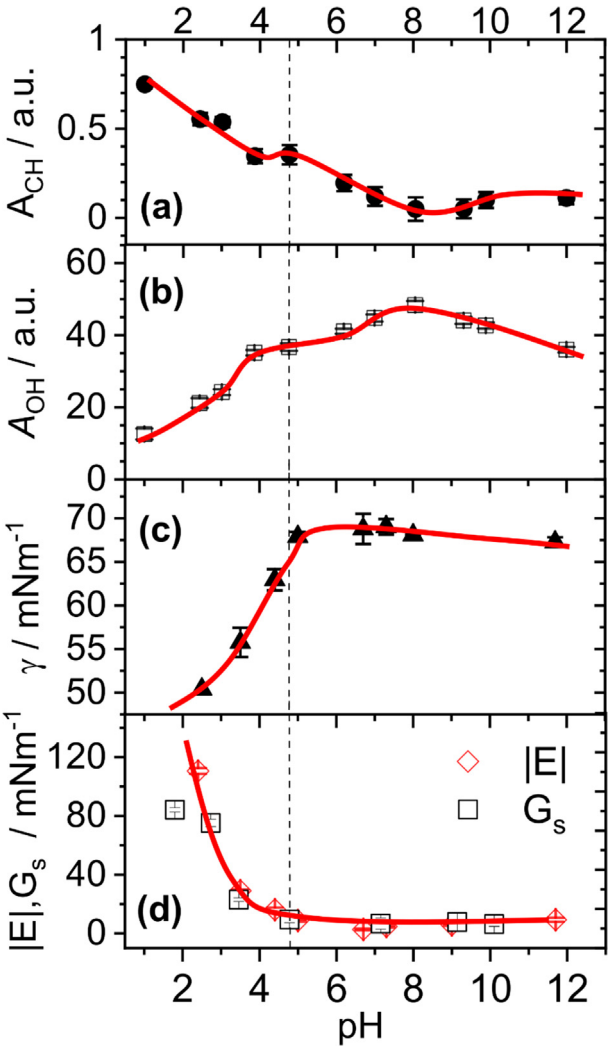

Fig. 4. SFG amplitudes as a function of pH of (a) the CH_2 symmetric stretching mode at ~ 2855 cm^{-1} and (b) the O—H band that were taken from the nonlinear least square fits to the SFG spectra in Fig. 2. (c) Shows the equilibrium interface tension of a 25 μM β-escin at the air-water interface as a function of pH while in (d) the interfacial dilatational visco-elasticity |E| (squares) (which need to be seen critical as discussed in the experimental details) and the surface elasticity G_s (red diamonds) are presented. Solid lines are guide the eye. Dashed line marks estimated pK [18] of the carboxylic acid group at the glycone of β-escin (see Fig. 1).

For pH values much lower than 4.7, the deprotonation of the carboxylic acid group of interfacial β-escin is reduced until the molecules are in an electrical neutral state at the air-water interface (pH < 3). This minimizes the double-layer contribution $\chi^{(3)}\phi_0$ to the O—H intensity and also the interface tension (Fig. 4b and 4c). This decrease of the interface tension with pH and surface charging state, is clearly related to the change in dominating intermolecular interactions at the air-water interface. Since at higher pH, repulsive interaction between interfacial β-escin molecules can be dominant, the molecules try to achieve a larger distance to neighboring molecules. This effectively decreases the surfactants' surface excess and, consequently, the interface tension. This conclusion is corroborated by previous surface tension and neutron reflectivity (NR) measurements [7] of β-escin adsorption layers at the air-water interface, where two selected pH values of 4 and 8 were studied. These were assumed to represent the neutral and fully ionized forms of β-escin. At pH 8 and a β-escin concentration of 30 μM, which is close to the concentration of 25 μM used in our study, a surface excess of 1.8 μmol/m^2 is seen by NR. When the pH was set to 4 the surfaces excess increased to 2.4 μmol/m^2.[7] Furthermore, the rise in interface tension e.g. between pH 4 and 8 from 60 to 68 mN/m as observed in our pendant drop experiments, is consistent to what Penfold et al. [7] reported in their study, where the authors have applied the Wilhelmy plate method to determine the interface tension. Fig. 4d shows the dramatic increase in surface dilatational elasticity |E| and the surface elasticity G_s (see Experimental Details) at low pH. Although we must point out that |E| as determined from the oscillating drop experiments is likely impaired by rather fast changes of the surface area with respect to the long relaxation times of the adsorbate layer as explained in detail in the experimental details section, |E| and G_s follow the same trend as a function of pH which can be qualitatively related to the reduction of electrostatic repulsion as was indirectly evidenced by our SFG results above. Consequently, dominating attractive intermolecular interactions at the air-water interface occur, when the pH is low enough ($\ll$5). In particular, Tsibranska et al. [17] have pointed out that attractive hydrophobic interactions of the aglycones of interfacial β-escin, as well as, dipole–dipole interactions and strong short-range hydrogen bonds between the sugar residues of β-escin can be relevant. Here, we note that the remarkable surface rheology of saponins has been subject to many excellent previous works [3,5,21] to which the reader is referred to for a more detailed discussion. We take the changes in Fig. 4d as further evidence for our conclusion on the differences in interfacial intermolecular interactions and surface excess when comparing low and high pH values (see above).

Instead we now want to shift the discussion to another important property of β-escin adsorption layers, that is the molecular orientation of interfacial β-escin and its change with pH. Some

insight into possible orientations was already reported in the MD simulation study by Tsibranska et al.[9,17], who have addressed the self-assembly of the neutral and charged forms of β-escin. In order to study possible orientation changes, we will now discuss the C—H modes in the frequency region from 2800 to 3100 cm^{-1} (Fig. 2b) in more detail. A close inspection of Fig. 2b and 4a shows that the SFG amplitude of the C—H bands and change in addition to the already discussed O—H stretching bands, which have been attributed to the change in interfacial charging state as the carboxylic acid group of β-escin gets deprotonated at high pH. This is different for the C—H bands where such electric-field induced components are negligible as shown by many previous studied that have addressed surfactants[25,36], polyelectrolytes[37], proteins[38,39] and other charged amphiphiles[40].

Thus, the drastic changes of the SFG amplitude of C—H bands in Fig. 2b and 4a and can be attributed to coverage and orientational changes of the β-escin surfactants at the air-water interface when the pH is increased from acidic values. At the interface, the neutral form prevails at low pH while at basic pH values the fully deprotonated form of β-escin dominates the air-water interface. At pH 2.4, the SFG spectrum in Fig. 2b is dominated by three strong bands at 2855, 2930–2945 and 2977 cm^{-1}, which we attribute to symmetric CH_2 stretching vibration (d^+), Fermi resonance of the symmetric (r^+-FR) as well as to CH_3 antisymmetric stretching vibrations (r^-), respectively [41,42]. In addition to the strong bands, at pH below 3.9, a much weaker band at 2904 cm^{-1} can be noticed as a shoulder of the r^+-FR. We attribute this weak band at 2904 cm^{-1} to C—H stretching vibrations of methine groups or the CH at the aglycone of β-escin while also the Fermi resonance of CH_2 symmetric stretch (d^+-FR) might be also contributing here. At low pH with the neutral form of β-escin dominating the air-water interface the C—H intensity is higher than at higher pH (Fig. 2a and 4a), where the charged form of β-escin is the prevailing interfacial species. This interesting result must be related to a change in the molecular orientation of β-escin at the air-water interface. Tsibranska et al.[17] discussed in their work two possible scenarios where they have studied β-escin with MD simulation: one with a low surface coverage that could be linked to the charged form and another one with high surface coverage that can be linked to the charge neutral form of β-escin at the interface (see also Fig. 5). They demonstrated that the angle which describes the tilt of the aglycone versus the surface normal is different for the low and the high surface coverage (2.4 vs 3.4 μmol/m^2), but also showed a rather broad angle distribution in both cases. For the high surface coverage, the net orientation of the aglycone show smaller tilt angle with aglycone nearly perpendicular to the surface while at very dilute conditions, β-escin was reported to be adsorbed to the interface with the aglycone in a geometry that is rather parallel to the surface plane.[9]

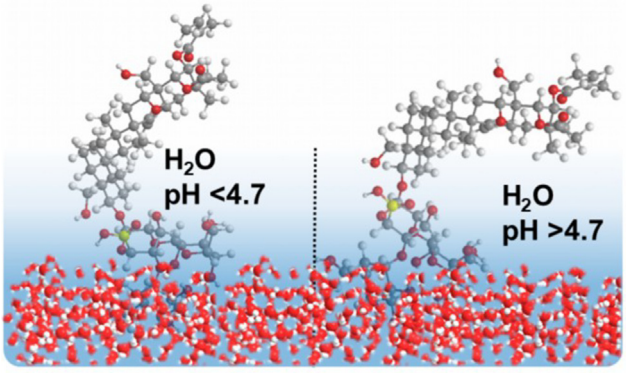

Fig. 5. Schematic drawing of the proposed molecular structure transformation of the β-escin modified air-water interfaces at low and high pH.

This agrees with the changes in C—H modes in our SFG spectra, where higher amplitudes are related to more ordered and more closed-packed β-escin molecules adsorbed at the air/water interface. According to the results of the NR study by Penfold et al.,[7] the surface excess is always at or below 2.4 μmol/m^2, while the thickness of the hydrophobic part of the adsorption layer is with 0.8 nm much smaller than the expected length (1.4 nm) of this part of the molecule. Assuming a tilted geometry, a tilt angle vs the surface normal of 55° can be calculated from simple geometric consideration, which is mostly consistent with what Tsibranska et al.[17] have reported for the system with a coverage of 2.4 μmol/m^2. Taking these earlier reports and considerations into account we propose that β-escin reorients at the air-water interface at low pH < 3 in a more upright geometry that can be more perpendicular to the surface with a smaller tilt angle. While at more basic pH the surface coverage decreases, whereas the tilt angle increases. These different geometries, suggested by earlier reports, are in qualitative agreement with the observed changes in C—H stretching modes. At low pH, one can expect that the preferred adsorption geometry leads to a higher preferentially alignment of the CH_2 groups in a direction perpendicular to the surface plane while at basic pH the changes in adsorption geometry, and possibly in the tilt angle, aligns the CH_3 groups more perpendicular to the surface plane and the intensity of the r^+ and the r^+-FR do not vanish so drastically as for the d^+ and d^+-FR modes (Fig. S2 in the Supporting Information for better comparison). In addition, a frequency shift of >13 cm^{-1} is observed for the 2930 cm^{-1} mode (r^+-FR) as a function of pH (Fig. S3). This frequency shift accompanies the same trend as observed for all other parameters in Fig. 4. The dominating attractive intermolecular interactions at the interface at lower pH, previously discussed, can affect the vibrational coupling and the energy transfer between the CH_3 stretching modes and the neighboring molecules.

6. Summary and conclusions

In this study we have addressed the change in molecular structure and charge state of the biosurfactant β-escin at the air-water interface using vibrational sum-frequency generation (SFG), surface tensiometry and surface dilational rheology. SFG spectra of β-escin modified air-water interface show that the intensity of O—H stretching vibrations of interfacial water molecules is a function of the bulk pH. At low pH values pH < 4, very low O—H intensities are observed while at higher pH values the O—H intensity is drastically increased and reaches a plateau value at pH > 6. These substantial changes in the O—H spectra are accompanied by substantial changes in C—H bands from interfacial β-escin moieties.

The change in O—H stretching modes is associated to electric-field induced third-order contributions to the SFG intensity, which are directly dependent on the double-layer potential at the interface. The power of SFG spectroscopy to address interface charging is well-known and has been used also for studies of other charged interfaces that were modified by surfactants, proteins and polyelectrolytes, just to mention a few systems. For that reason, we have applied SFG spectroscopy to address surface charging of β-escin adsorption layers at the air-water interface by studying the change in O—H intensity with the bulk pH value. At very low pH of < 4, we have concluded from our analysis of the SFG spectra that the interfacial β-escin moieties are adsorbed in their charge neutral form, while at higher pH > 6 the carboxylic acid group of β-escin is deprotonated and fully ionized. This interfacial charging behavior is largely consistent with what has been reported in the bulk solution, where the carboxylic acid group of β-escin was titrated.[18]

The differently charged surfaces also cause changes in the equilibrium surface tension, which increases when the solutions' pH is increased to a value > 2 and also plateaus at pH > 6. The trends in the changes in surface tension and O—H intensity are in excellent agreement, which suggests that the change in intermolecular interactions at the air-water interface from low pH < 4 to higher pH > 6 changes from an attractive regime that is dominated by hydrophobic interactions and hydrogen bonding to a repulsive regime where electrostatic interactions become more dominant as was evidenced by SFG spectroscopy at the air-water interface. These changes in interactions at the air-water interface are the origin of the different surface excess of β-escin and, thus, the different equilibrium surface tension as well as the huge differences in surface dilational elasticity. In fact, the surface elasticity drastically increases once the charging of the interfacial layer of β-escin is reduced by lowering the solution pH and yields the remarkable behavior in surface rheology that is already known for saponins.

In addition to the changes in surface charging, also the structural arrangement of β-escin is a function of the solutions' pH, where the change in structure is clearly related to tighter packing of β-escin at the air-water interface when the surface net charge is negligible.

CRediT authorship contribution statement

Dana Glikman: Investigation, Data curation, Validation. **Natalia García Rey:** Investigation, Formal analysis, Writing – original draft. **Manuela Richert:** Investigation. **Konrad Meister:** Conceptualization. **Björn Braunschweig:** Conceptualization, Methodology, Writing – review & editing, Supervision, Project administration, Funding acquisition, Resources, Visualization.

Declaration of Competing Interest

The authors declare that they have no known competing financial interests or personal relationships that could have appeared to influence the work reported in this paper.

Acknowledgments

The authors gratefully acknowledge funding from the European Research Council (ERC) under the European Union's Horizon 2020 research and innovation program (Grant Agreement 638278).

Appendix A. Supplementary material

Supplementary data to this article can be found online at https://doi.org/10.1016/j.jcis.2021.09.086.

References

[1] J.M.R. Patlolla, C.V. Rao, Anti-inflammatory and anti-cancer properties of β-escin, a triterpene saponin, Curr. Pharmacol. Rep. 1 (3) (2015) 170–178.
[2] D. Domanski, O. Zegrocka-Stendel, A. Perzanowska, M. Dutkiewicz, M. Kowalewska, I. Grabowska, D. Maciejko, A. Fogtman, M. Dadlez, K. Koziak, Molecular mechanism for cellular response to B-escin and its therapeutic implications, Plos One 11 (2016) E0164365.
[3] K. Golemanov, S. Tcholakova, N. Denkov, E. Pelan, S.D. Stoyanov, Surface shear rheology of saponin adsorption layers, Langmuir 28 (33) (2012) 12071–12084.
[4] N. Pagureva, S. Tcholakova, K. Golemanov, N. Denkov, E. Pelan, S.D. Stoyanov, Surface properties of adsorption layers formed from triterpenoid and steroid saponins, Coll. Surf. A 491 (2016) 18–28.
[5] K. Golemanov, S. Tcholakova, N. Denkov, E. Pelan, S.D. Stoyanov, Remarkably high surface visco-elasticity of adsorption layers of triterpenoid saponins, Soft Matter 9 (24) (2013) 5738, https://doi.org/10.1039/c3sm27950b.
[6] G. Giménez-Ribes, M. Habibi, L.M.C. Sagis, Interfacial rheology and relaxation behavior of adsorption layers of the triterpenoid saponin escin, J. Coll. Int. Sci. 563 (2020) 281–290.
[7] J. Penfold, R.K. Thomas, I. Tucker, J.T. Petkov, S.D. Stoyanov, N. Denkov, K. Golemanov, S. Tcholakova, J.R.P. Webster, Saponin adsorption at the air-water interface-neutron reflectivity and surface tension studY, Langmuir 34 (32) (2018) 9540–9547.
[8] S. Tcholakova, F. Mustan, N. Pagureva, K. Golemanov, N.D. Denkov, E.G. Pelan, S.D. Stoyanov, Role of surface properties for the kinetics of bubble ostwald ripening in saponin-stabilized foams, Coll. Surf. A 534 (2017) 16–25.
[9] S. Tsibranska, A. Ivanova, S. Tcholakova, N. Denkov, Self-assembly of escin molecules at the air-water interface as studied by molecular dynamics, Langmuir 33 (33) (2017) 8330–8341.
[10] E. Santini, E. Jarek, F. Ravera, L. Liggieri, P. Warszynski, M. Krzan, Surface properties and foamability of saponin and saponin-chitosan systems, Coll. Surf. B 181 (2019) 198–206.
[11] S. Tsibranska, S. Tcholakova, K. Golemanov, N. Denkov, E. Pelan, S.D. Stoyanov, Role of interfacial elasticity for the rheological properties of saponin-stabilized emulsions, J. Coll. Int. Sci. 564 (2020) 264–275.
[12] R. Geisler, C. Dargel, T. Hellweg, The biosurfactant β-aescin: a review on the physico-chemical properties and its interaction with lipid model membranes and langmuir monolayers, Molecules 25 (1) (2020) 117.
[13] R. Geisler, M.C. Pedersen, N. Preisig, Y. Hannappel, S. Prévost, R. Dattani, L. Arleth, T. Hellweg, Aescin – a natural soap for the formation of lipid nanodiscs with tunable size, Soft Matter 17 (7) (2021) 1888–1900.
[14] R. Geisler, M.C. Pedersen, Y. Hannappel, R. Schweins, S. Prévost, R. Dattani, L. Arleth, T. Hellweg, Aescin-induced conversion of gel-phase lipid membranes into bicelle-like lipid nanoparticles, Langmuir 35 (49) (2019) 16244–16255.
[15] I.M. Tucker, A. Burley, R.E. Petkova, S.L. Hosking, J. Penfold, R.K. Thomas, P.X. Li, J.R.P. Webster, R. Welbourn, Mixing natural and synthetic surfactants: co-adsorption of triterpenoid saponins and sodium dodecyl sulfate at the air-water interface, Langmuir 36 (21) (2020) 5997–6006.
[16] I.M. Tucker, A. Burley, R.E. Petkova, S.L. Hosking, R.K. Thomas, J. Penfold, P.X. Li, K. Ma, J.R.P. Webster, R. Welbourn, Surfactant/biosurfactant mixing: adsorption of saponin/nonionic surfactant mixtures at the air-water interface, J. Coll. Int. Sci. 574 (2020) 385–392.
[17] S. Tsibranska, A. Ivanova, S. Tcholakova, N. Denkov, Structure of dense adsorption layers of escin at the air–water interface studied by molecular dynamics simulations, Langmuir 35 (39) (2019) 12876–12887.
[18] C. Dargel, R. Geisler, Y. Hannappel, I. Kemker, N. Sewald, T. Hellweg, Self-assembly of the bio-surfactant aescin in solution: a small-angle x-ray scattering and fluorescence study, Coll. Interfaces 3 (2019) 47.
[19] A. Javadi, N. Mucic, M. Karbaschi, J.Y. Won, M. Lotfi, A. Dan, V. Ulaganathan, G. Gochev, A.V. Makievski, V.I. Kovalchuk, N.M. Kovalchuk, J. Krägel, R. Miller, Characterization methods for liquid interfacial layers, Eur. Phys. J. SpecTop. 222 (1) (2013) 7–29.
[20] R. Stanimirova, K. Marinova, S. Tcholakova, N.D. Denkov, S. Stoyanov, E. Pelan, Surface rheology of saponin adsorption layers, Langmuir 27 (20) (2011) 12486–12498.
[21] V. Ulaganathan, L. Del Castillo, J.L. Webber, T.T. Ho, J.K. Ferri, M. Krasowska, D. A. Beattie, The influence of ph on the interfacial behaviour of quillaja bark saponin at the air-solution interface, Coll. Surf. B 176 (2019) 412–419.
[22] A.D. Cramer, W.-F. Dong, N.L. Benbow, J.L. Webber, M. Krasowska, D.A. Beattie, J.K. Ferri, The influence of polyanion molecular weight on polyelectrolyte multilayers at surfaces: elasticity and susceptibility to saloplasticity of strongly dissociated synthetic polymers at fluid–fluid interfaces, Phys. Chem. Chem. Phys. 19 (2017) 23781–23789.
[23] Y.R. Shen, Surface properties probed by second-harmonic and sum-frequency generation, Nature 337 (6207) (1989) 519–525.
[24] G. Gonella, C. Lütgebaucks, A.G.F. de Beer, S. Roke, Second harmonic and sum-frequency generation from aqueous interfaces is modulated by interference, J. Phys. Chem. C 120 (17) (2016) 9165–9173.
[25] N. García Rey, E. Weißenborn, F. Schulze-Zachau, G. Gochev, B. Braunschweig, Braunschweig, quantifying double-layer potentials at liquid-gas interfaces from vibrational sum-frequency generation, J. Phys. Chem. C 123 (2) (2019) 1279–1286.
[26] P.E. Ohno, H.-F. Wang, F.M. Geiger, Second-order spectral lineshapes from charged interfaces, Nat. Comm. 8 (1) (2017) 1032.
[27] F. Tang, T. Ohto, S. Sun, J.R. Rouxel, S. Imoto, E.H.G. Backus, S. Mukamel, M. Bonn, Y. Nagata, Molecular structure and modeling of water–air and ice–air interfaces monitored by sum-frequency generation, Chem. Rev. 120 (8) (2020) 3633–3667.
[28] Y.R. Shen, V. Ostroverkhov, Sum-frequency vibrational spectroscopy on water interfaces: polar orientation of water molecules at interfaces, Chem. Rev. 106 (2006) 1140–1154.
[29] D.K. Hore, E. Tyrode, Probing charged aqueous interfaces near critical angles: effect of varying coherence length, J. Phys. Chem. C 123 (27) (2019) 16911–16920.
[30] M.S. Azam, C. Cai, J.M. Gibbs, E. Tyrode, D.K. Hore, Silica surface charge enhancement at elevated temperatures revealed by interfacial water signals, J. Am. Chem. Soc. 142 (2) (2020) 669–673.
[31] B. Rehl, M. Rashwan, E.L. Dewalt-Kerian, T.A. Jarisz, A.M. Darlington, D.K. Hore, J.M. Gibbs, New insights into $\chi^{(3)}$ measurements: comparing nonresonant second harmonic generation and resonant sum frequency generation at the silica/aqueous electrolyte interface, J. Phys. Chem. C 123 (17) (2019) 10991–11000.
[32] D.E. Gragson, G.L. Richmond, Investigations of the structure and hydrogen bonding of water molecules at liquid surfaces by vibrational sum frequency spectroscopy, J. Phys. Chem. B 102 (20) (1998) 3847–3861.

[33] Y. Nagata, S. Mukamel, Vibrational sum-frequency generation spectroscopy at the water/lipid interface: molecular dynamics simulation study, J. Am. Chem. Soc. 132 (18) (2010) 6434–6442.
[34] T. Ohto, E.H.G. Backus, C.-S. Hsieh, M. Sulpizi, M. Bonn, Y. Nagata, Lipid carbonyl groups terminate the hydrogen bond network of membrane-bound water, J. Phys. Chem. Lett. 6 (22) (2015) 4499–4503.
[35] Y. Nojima, Y. Suzuki, S. Yamaguchi, Weakly hydrogen-bonded water inside charged lipid monolayer observed with heterodyne-detected vibrational sum frequency generation spectroscopy, J. Phys. Chem. C 121 (4) (2017) 2173–2180.
[36] E. Tyrode, R. Corkery, Charging of carboxylic acid monolayers with monovalent ions at low ionic strengths: molecular insight revealed by vibrational sum frequency spectroscopy, J. Phys. Chem. C 122 (50) (2018) 28775–28786.
[37] F. Schulze-Zachau, S. Bachmann, B. Braunschweig, Effects of ca^{2+} ion condensation on the molecular structure of polystyrene sulfonate at air-water interfaces, Langmuir 34 (39) (2018) 11714–11722.
[38] M.E. Richert, G.G. Gochev, B. Braunschweig, Specific ion effects of trivalent cations on the structure and charging state of B-lactoglobulin adsorption layers, Langmuir 35 (35) (2019) 11299–11307.
[39] S. Hosseinpour, S.J. Roeters, M. Bonn, W. Peukert, S. Woutersen, T. Weidner, Structure and dynamics of interfacial peptides and proteins from vibrational sum-frequency generation spectroscopy, Chem. Rev. 120 (7) (2020) 3420–3465.
[40] M. Schnurbus, R.A. Campbell, J. Droste, C. Honnigfort, D. Glikman, P. Gutfreund, M.R. Hansen, B. Braunschweig, Photo-switchable surfactants for responsive air–water interfaces: azo versus arylazopyrazole amphiphiles, J. Phys. Chem. B 124 (2020) 6913–6923.
[41] R. Lu, W. Gan, B.-H. Wu, Z. Zhang, Y. Guo, H.-F. Wang, C−H Stretching vibrations of methyl, methylene and methine groups at the vapor/alcohol (n = 1–8) interfaces, J. Phys. Chem. B 109 (29) (2005) 14118–14129.
[42] E. Tyrode, J. Hedberg, A comparative study of the cd and ch stretching spectral regions of typical surfactants systems using vsfs: orientation analysis of the terminal CH_3 and CD_3 groups, J. Phys. Chem. C 116 (1) (2012) 1080–1091.